

PHASE DRIFT IN A MULTISTAGE KLYSTRON-LIKE FREE-ELECTRON LASER

KEN TAKAYAMA*

*Institute for Beam Particle Dynamics, University of Houston,
Houston, Texas 77204-5506, USA and Texas Accelerator Center,
The Woodlands, Texas 77381, USA*

(Received 13 May 1991; in final form 24 September 1991)

The sensitivity of RF phase to current and energy errors in a multistage klystron-like free-electron laser is analyzed theoretically, using the macroparticle approach. Theoretical results are confirmed by comparison with numerical simulations and the importance of detrapped beam fraction is noted. An example of gigantic K-band RF source with output power of 600 MW/m and total length of 150 m is given. This is shown to have an acceptable phase sensitivity for 100 multistages.

1 INTRODUCTION

Since the first proposal of a two-beam accelerator¹ based on free-electron lasers (TBA/FEL) by Sessler, its output RF phase's sensitivity to injection errors has been one of principal key issues for a practical RF source of a future TeV class linear collider. Although the new version² of TBA/FEL (TBA/KFEL)³ seems to eliminate the complicated RF phase control⁴ as proposed in the original version, there has been no work which clearly show physical insight into this problem in the TBA/KFEL.

Pulse-to-pulse phase drift caused by injection jitters in beam current or energy has been independently considered by LBL/MIT⁵ and KEK⁶ in a conceptually similar framework which may be called the macroparticle approach³. Introducing three single-period functions determined by numerically integrating the single particle FEL equations of motion and linearizing them with respect to displacement from the designed values, the former has evaluated a set of linear evolution equations for phase and given a condition for less sensitiveness. One example of single particle FEL simulations which supports the theory has been presented in Ref. 5. Unfortunately, it is not so easy to find the FEL parameter dependence of phase drift, by using this theory. Employing the universal gain function introduced in Ref. 3, meanwhile, Takayama has attempted to develop a full set of evolution equations for energy, ponderomotive phase, and output RF phase in the recursion form with a mathematically much simpler structure. The attempt of Ref. 6 has been not completed because

*On leave from National Laboratory for High Energy Physics in Japan (KEK).

the dependence of the universal gain function on the initial value of ponderomotive phase was ignored.

In this article, a theory as a further development of the original idea⁶ is presented which delineates the spatial-evolution of beam energy, ponderomotive phase, and output RF phase from period to period in a set of recursion forms. The model is based on the macroparticle approach (MPA) in Ref. 3 which is briefly summarized in Section 2.

The model is applied to the case of well bunched beam where an injected beam current is conserved through more than 100 periods. The set of coupled recursion equations is exactly solved and its solution is compared with the spatial evolution of bunch center and output RF phase by multiparticle simulations (MUS)⁷. As a result, steady-state characteristics of this case is elucidated in an equilibrium solution for the set of recursion equations. The RF phase's sensitivity to injection errors such as possible current error is assessed, based on the equilibrium solution and shown to be consistent with results of the realistic MUS. In addition, the theory will give a clear answer to the unsolved question how the output RF phase's sensitivity to injection errors depends on the magnitude of input RF power.

An important aspect that the output RF phase rapidly changes because of a sizable amount of current loss due to longitudinal mismatching in the early transient stages of a TBA/KFEL where bunching still does not evolve sufficiently is pointed out as a result of the realistic MUS. The necessity of a long buncher section for a desired TBA/KFEL is suggested.

2 MACROPARTICLE MODEL AND UNIVERSAL GAIN EQUATION

In the KFEL, a small RF signal is fed in at the start of each period and amplified by the FEL. Near the end of period the RF signal is removed. The electrons of the driving beam go on from period to period. It is noted that the signal phase is well adjusted at the injection of each stage, as mentioned later. Motion of the particles through a period may be well understood by the concept of synchrotron oscillation: At the initial stage of the period, the injected RF amplitude is small and most of the particles are outside a bucket. The rapidly increasing RF bucket begins to capture the particles performing synchrotron oscillation. After RF extraction, the particles enter into the energy recovery section with a small acceleration gap at its ends. Their motion in this section is characterized by drift along the ponderomotive phase axis and abrupt energy change.

A magnitude of the amplified RF signal is dominated by the overall behavior of the particles; the RF wave in the KFEL strongly couples with the collective motion of the particles. In the MPA, the behavior of the bunch center is assumed to represent a collective motion of the bunch and the bunch center has been called the macroparticle (MP).

We consider the motion of an electron in the planar wiggler field which is characterized by wiggler wave number k_w and normalized wiggler field b_w . The electron is strongly coupled with the RF field which is characterized by wave number

k_s and angular frequency ω_s . FEL equations for the MP have been originally given in Ref. 3 which can be straightforwardly written from the standard FEL formulation⁸. The field equations are written in terms of slowly evolving normalized amplitude e_s and phase shift ϕ_s of the signal wave. The particle equations describe the motion of the MP which is represented by terms of energy γ_a in rest-mass units and ponderomotive phase $\phi_a = (k_s + k_w)z - \omega_s t + \phi_s$. The MP FEL equations for a TE_{01} mode in a rectangular waveguide ($a^* \times b^*$) are

$$\frac{d\gamma_a}{dz} = -\frac{e_s b_w}{k_w \gamma_a} \sin \phi_a \quad (1a)$$

$$\frac{d\phi_a}{dz} = k_w - \delta k_s - \frac{1}{2\gamma_a^2} \left[\frac{\omega_s}{c} \right] \left(1 + \left[\frac{b_w}{k_w} \right]^2 \right) + \frac{d\phi_s}{dz} \quad (1b)$$

$$\frac{de_s}{dz} = \frac{eZ_0}{2mc^2} \left[\frac{b_w}{k_w} \right] \kappa J \frac{\sin \phi_a}{\gamma_a} \quad (1c)$$

$$\frac{d\phi_s}{dz} = \frac{eZ_0}{2mc^2} \left[\frac{b_w}{k_w} \right] \frac{\kappa J \cos \phi_a}{e_s \gamma_a} \quad (1d)$$

$$\kappa = \frac{\sin \Delta\phi}{\Delta\phi}, \quad k_s = \left(\left[\frac{\omega_s}{c} \right]^2 - \left[\frac{\pi}{b^*} \right]^2 \right)^{1/2}$$

$$\delta k_s = \frac{\omega_s}{c} - k_s$$

where we assume the particles are initially bunched with half phase spread $\Delta\phi$, $J = 2I/a^*b^*$ (I : beam current) is the current density averaged over the effective area of the TE_{01} mode, and $Z_0(377 \Omega)$ is the value of resistance in vacuum. From (1c), we have straightforwardly

$$\phi_a = \sin^{-1} \left[\frac{\gamma_a}{\kappa K b_w} \dot{e}_s \right], \quad \left(\cdot \equiv \frac{d}{dz} \right) \quad (2)$$

where $K \equiv eZ_0 J / 2mc^2 k_w$. Differentiation of (2) with respect to z leads to

$$\dot{\phi}_a = \frac{1}{\cos \phi_a} \frac{d}{dz} \left[\frac{\gamma_a}{\kappa K b_w} \dot{e}_s \right] \quad (3)$$

Substituting (3) and (1d) into (1b), we obtain the second-order differential equation for e_s ,

$$\begin{aligned} \frac{d}{dz} \left[\frac{\gamma_a}{\kappa K b_w} \dot{e}_s \right] \simeq & \left[k_w - \delta k_s - \frac{1}{2} \left(\frac{\omega_s}{c} \right) \left(\frac{b_w}{\gamma_a k_w} \right)^2 \right] \left[1 - \left(\frac{\gamma_a}{\kappa K b_w} \dot{e}_s \right)^2 \right]^{1/2} \\ & + \left(\frac{\kappa K b_w}{\gamma_a e_s} \right) \left[1 - \left(\frac{\gamma_a}{\kappa K b_w} \dot{e}_s \right)^2 \right] \end{aligned} \quad (4)$$

where $a_w \equiv b_w/k_w \gg 1$ and $|\phi_a| \leq \pi/2$ are assumed. Equations (1a) and (1c) give an

invariant of motion,

$$\gamma_a + \frac{mc^2}{eZ_0 J\kappa} e_s^2 = \text{const.} \quad (5)$$

Once Eq. (4) is solved under the initial conditions, $e_s(0) = e_0$ and $\dot{e}_s(0) = (eZ_0 J a_w \kappa / 2mc^2)(\sin \phi_a(0) / \gamma_a(0))$, the motion of the MP is easily reconstructed from (2) and (5).

Introducing an assumption of implicit taper, $\gamma_a / K b_w \equiv a = \text{const}$, and the change of variables

$$x = [a|b|/\kappa]e_s, \quad s = |b|z \quad (6)$$

where

$$b = k_w - \delta k_s - \frac{1}{2} \left(\frac{\omega_s}{c} \right) \left[\frac{1}{k_w K a} \right]^2$$

Equation (4) reduces to

$$x'' = -[1 - (x')^2]^{1/2} + [1 - (x')^2]/x \quad (7)$$

$$\left(' \equiv \frac{d}{ds} \right)$$

By further transformation, $y = \ln x$, we arrive at the so-called universal gain equation (UGE),

$$y'' = -[e^{-2y} - (y')^2]^{1/2} + e^{-2y} - 2(y')^2 \quad (8)$$

with the initial conditions, $y(0) = \ln[a|b|e_s(0)/\kappa]$ and $y'(0) = (\kappa \sin \phi_a(0) / a|b|e_s(0))$. Its solution $y(s)$ has been called the universal gain function (UGF). Generic properties of the UGE and UGF have been in detail discussed in Ref. 3.

3 RECURSION FORMULA

Using the UGF, we can develop the recursion formula which describe the period-to-period evolution of the MP in the phase space and the output RF phase, as depicted in Figure 1. From the energy conservation law we have the discrete evolution equation for γ_a ,

$$\gamma_a^{n+1} = \gamma_a^n - \frac{\kappa}{4} \left[\frac{eZ_0 J}{mc^2} \right] \frac{a_w^2(0) \exp[2y(|b(\gamma_a^n)|L_w)]}{(\gamma_a^n)^2 |b(\gamma_a^n)|^2} + \Delta\gamma + \frac{e}{mc^2} \frac{P(0)}{I} \quad (9a)$$

where the second term in the right-hand side represents the energy converted to the RF power, the third term is the energy replenished at each accelerating gap depicted by I in Figure 1, the last term is proportional to the input RF power $P(0)$, and L_w denotes the wiggler length per period. The continuity⁹ of beam phase, $\theta = (k_s +$

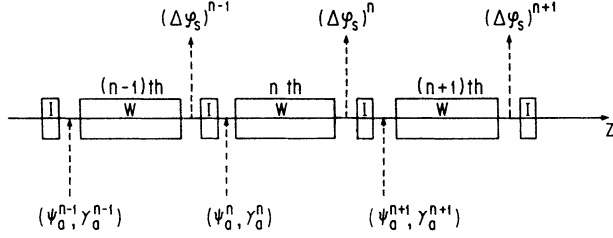


FIGURE 1 A sequence of regular wiggler and accelerating unit in a TBA/KFEL.

$k_w z - \omega_s t$, at boundary gives the discrete equation for ϕ_a ,

$$\phi_a^{n+1} = \theta_{out}^n + (\phi_s^{n+1})_{in}$$

By using the MP's variables, this relation is rewritten in the more convenient form,

$$\begin{aligned} \phi_a^{n+1} &= (\phi_a^n)_{out} - (\Delta\phi_s)^n + \Delta(\equiv (\phi_s^{n+1})_{in} - (\phi_s^n)_{in}) \\ &= \phi_a^n - |b(\gamma_a^n)|L_w + \Delta \end{aligned} \quad (9b)$$

where Δ is externally controlled by adjusting the input signal phase. Integrating the first-order differential equation (1d) for the signal phase, we have the increment in the RF phase through period,

$$(\Delta\phi_s)^n = \frac{I}{I_0} \int_0^{|b(\gamma_a^n)|L_w} \sqrt{e^{-2y(s)} - (y')^2} ds \quad (9c)$$

where I_0 is the designed beam current.

Assuming an input beam current error, $\Delta I = I - I_0$, the recursion formulae are written in the terms of the small deviation from the designed energy, $\delta_n = \gamma_a^n - \gamma_0$,

$$\delta_{n+1} = (1 - \mu)\delta_n + \alpha(\phi_a^n - \phi_a^0) - \Delta\gamma \frac{\Delta I}{I_0} + \frac{e}{mc^2} \frac{P(0)}{I_0} \quad (10a)$$

$$\phi_a^{n+1} = \phi_a^n + \beta\delta_n + (\Delta - s_0) \quad (10b)$$

$$(\Delta\phi_s)^n \simeq \left(1 + \frac{\Delta I}{I_0}\right) [-\phi_a^n - \beta f(s_0)\delta_n + \text{const.}] \quad (10c)$$

where

$$\beta = \frac{\omega_s}{c} \frac{a_w^2(0)}{\gamma_0^3}$$

$$s_0 = |b(\gamma_0)|L_w$$

$$\mu = \frac{2\Delta\gamma}{\gamma_0} \left[\gamma_0 \beta y'(s_0) + \frac{1 + \gamma_0^2/\gamma_s^2}{1 - \gamma_0^2/\gamma_s^2} \right], \quad \gamma_s^2 = \frac{1}{2} \left(\frac{\omega_s}{k_s} \right) \frac{a_w^2(0)}{k_w - \delta k_s}$$

$$f(s) \equiv \sqrt{e^{-2y(s)} - (y'(s))^2}$$

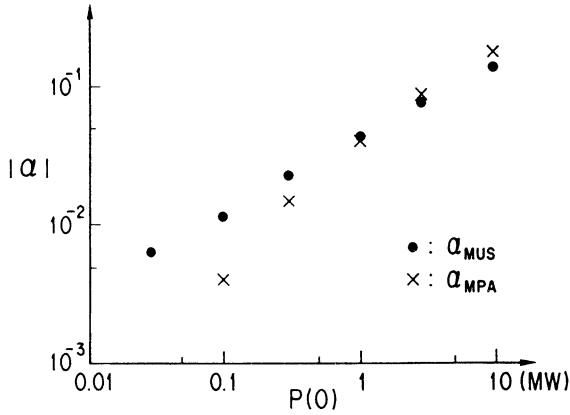


FIGURE 2 $|\alpha|$ vs. the input power $P(0)$ at $\phi_a^0 \sim 90^\circ$.

γ_s may be called the resonant energy in a formal sense. The expression for damping parameter μ has been evaluated in Ref. 3. The term related to ϕ_a^0 in (10a) is originated from the initial condition of the UGF, and the coefficient α must be numerically determined. It is noted that α depends on the input RF power because of $e_s(0) \propto \sqrt{P(0)}$. Figure 2 shows the absolute value of α derived from the MPA and obtained by the MUS as a function of the input power for the FEL parameters listed in Table 1, which are referred by α_{MPA} and α_{MUS} , respectively. Both α s agree to each other within a factor of two in a large scale. In the figure, the smallness of α in magnitude is notable for the kilowatt input power level. This simply means the almost one-way coupling between γ_a and ϕ_a in such low input power level. The feature is serious in a practical RF source, as will be discussed later.

TABLE 1
FEL Parameters

Injection beam current for a well bunched beam for an unmatched beam	I_0	1.802 kA 3.0 kA
Beam energy	$mc^2\gamma_0$	12.1 MeV
Energy gain per period	$mc^2\Delta\gamma$	0.5 MeV
Wiggler field	$\frac{\sqrt{2}mc}{e} b_w$	3.85 – 3.6 kG
Wiggler wave length	$2\pi/k_w$	0.26 m
Wiggler length per period	L_w	0.7 m
RF frequency	$\omega_s/2\pi$	17.1 GHz
RF input power	$P(0)$	10 MW
RF output power	$P(L_w)$	900 MW
Waveguide dimension	$a^* \times b^*$	$0.2 \times 0.03 \text{ m}^2$
Phase control parameter for a well bunched beam for an unmatched beam	Δ	3.405 3.0 (stage 1–11) 3.27 (stage 12–29) 3.33 (stage 30–100)

The validity of the recursion form has been confirmed by comparison with the MUS for a typical example, FEL parameters of which are given in Table 1. Two cases of 10 MW and 100 kW as the input power have been chosen which give the relatively large and small α . A δ -function like error in energy is introduced at the 50th stage. Then, the evolution in the resultant energy deviation, ponderomotive phase, and output RF phase are calculated over 50 stages downstream there. The behavior of γ_a^n , ϕ_a^n and $(\Delta\phi_s)^n$ predicted from (10a), (10b), (10c) was shown to be qualitatively and quantitatively in good agreement with the result of the MUS for both cases. The comparison in the case of the large input power is given in Figures 3a,b.

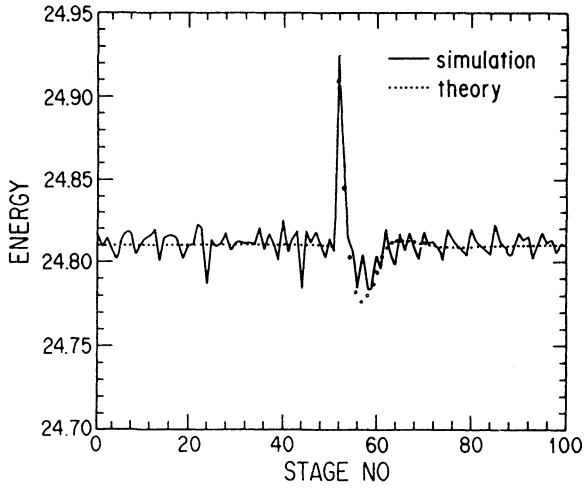


FIGURE 3a Energy deviation vs. the stage number.

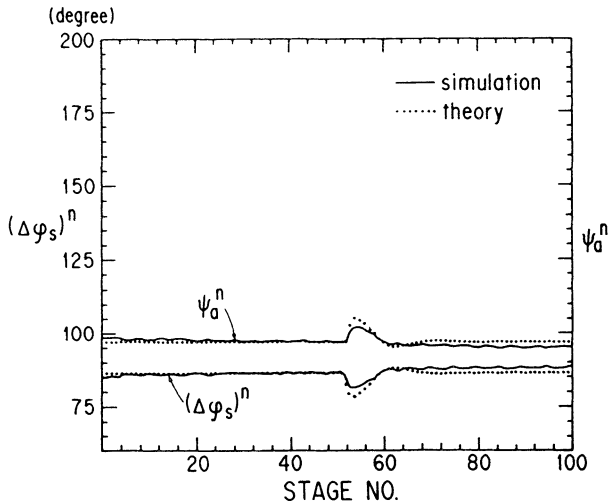


FIGURE 3b $(\Delta\phi_s)^n$ and ψ_a^n vs. the stage number.

4 PHASE DRIFT

In order to analytically estimate effects of the injection errors, we solve the coupled recursion equations (10a) and (10b); introducing $\chi_n = \phi_a^n - \phi_a^0$, their solutions are given by

$$\delta_n = \frac{1}{q_2 - q_1} [p - \dot{p} + (q_2^{n-1} - q_1^{n-1})\delta_2 - (q_2^{n-1}q_1 - q_1^{n-1}q_2)\delta_1 - (pq_2^{n-1} - \dot{p}q_1^{n-1})] \quad (11a)$$

$$\chi_n = \frac{1}{q_2 - q_1} [r - \dot{r} + (q_2^{n-1} - q_1^{n-1})\chi_2 - (q_2^{n-1}q_1 - q_1^{n-1}q_2)\chi_1 - (rq_2^{n-1} - \dot{r}q_1^{n-1})] \quad (11b)$$

with

$$\delta_2 = (1 - \mu)\delta_1 + \alpha\chi_1 - \Delta\gamma \frac{\Delta I}{I_0} + \frac{e}{mc^2} \frac{P(0)}{I_0} \quad (12)$$

$$p = -\frac{\alpha(\Delta - s_0)}{q_2 - 1}, \dot{p} = p \frac{q_2 - 1}{q_1 - 1} \quad (13)$$

$$r = -\frac{\mu(\Delta - s_0) + \beta[-\Delta\gamma\Delta I/I_0 + (e/mc^2)P(0)/I_0]}{q_2 - 1}, \dot{r} = r \frac{q_2 - 1}{q_1 - 1} \quad (14)$$

where q_1 and q_2 are solutions of the quadratic equation,

$$x^2 - (2 - \mu)x + (1 - \mu - \alpha\beta) = 0.$$

In a case of $|\alpha| < \mu^2/4\beta$, $q_1 (< 1) = 1 - \mu - \alpha\beta/\mu + O(\alpha^2)$ and $q_2 (< 1) = 1 + \alpha\beta/\mu + O(\alpha^2)$. For the case of the input power less than 100 kW where $|\alpha| < 10^{-2}$ as shown in Figure 2, the magnitudes of μ and β are of order of half of unity and unity, respectively. Thus, q_2 takes a value very close to unity. This results in a long damping time which may be beyond a desired stage number. This discouraging feature has been really observed in the MUS. Setting q_1^n in (11a) and (11b) to be zero and substituting into (10c), we have $(\Delta\varphi_s)^n$ in the terms of q_2^n ,

$$(\Delta\varphi_s)^n = (\Delta\varphi_s)_{\Delta I=0}^n + \left[(\Delta\varphi_s)_{\Delta I=0}^n + \beta\Delta\gamma \left\{ \frac{1}{\alpha\beta} (-1 + q_2^{n-1}) + \frac{f(s_0)}{\mu} q_2^{n-1} \right\} \right] \frac{\Delta I}{I_0} \quad (15)$$

where the terms originating from the current error are isolated in the bracket. In most of cases, the first term in the brace is dominant; in the limit of $\alpha \rightarrow 0$,

$$(\Delta\varphi_s)^n = (\Delta\varphi_s)_{\Delta I=0}^n + \frac{\beta\Delta\gamma}{\mu} (n-1) \frac{\Delta I}{I_0}, \left(n < 1 + \frac{\mu}{\alpha\beta} \right) \quad (16)$$

Accordingly, it turns out that the phase drift of the output RF caused by the current error at injection linearly grows with stage number up to some extent. This fact seriously limits a possible stage number or an acceptable size of the current error.

Since in practice we require a high number of stages and a large tolerance in current error, the case of low input power is ruled out in the following discussions.

Meanwhile, in the case of $|\alpha| > \mu^2/4\beta$, q_1 and q_2 are a pair of complex conjugate. Their absolute value $|q_1| = |q_2| = (1 - \mu - \alpha\beta)^{1/2}$ is much less than unity for the megawatt input power level where $|\alpha| \sim 10^{-1}$ as shown in Figure 2; therefore, δ_n and ϕ_a^n damp to reach to an equilibrium state,

$$\delta_\infty = \frac{p - \dot{p}}{q_2 - q_1} = -\frac{\Delta - s_0}{\beta} \quad (17)$$

$$\phi_a^\infty = \phi_a^0 - \frac{1}{\alpha\beta} \left[\mu(\Delta - s_0) + \beta \left\{ -\Delta\gamma \frac{\Delta I}{I_0} + \frac{e}{mc^2} \frac{P(0)}{I_0} \right\} \right] \quad (18)$$

A problem which arises at this point is that the above equilibrium state scatters shot by shot. The output RF phase determined by (10c) which is a function of δ_n and ϕ_a^n will scatter in the similar way. To manifest the sensitivity of the output RF phase to injection current error ΔI , the steady-state output RF phase is described in the similar form to that of the previous case, Eq. (16),

$$(\Delta\varphi_s)^\infty = (\Delta\varphi_s)_{\Delta I=0}^\infty + \left[(\Delta\varphi_s)_{\Delta I=0}^\infty - \frac{\Delta\gamma}{\alpha} \right] \frac{\Delta I}{I_0} \quad (19)$$

The theoretical prediction from Eq. (19) for the example of Table 1 which gives $\mu = 0.65$, $\alpha_{\text{MUS}} = -0.13(\alpha_{\text{MPA}}) = -0.18$, and $\beta = 1.0704$ is compared with results of the MUS in Figure 4. In most cases, the magnitude of the first term in the bracket of (19) is much smaller than that of the second term; in the example it is actually negligible. Substituting of $\Delta\gamma = 1$ and $\alpha = -0.18$ into the expression, we have the gradient of $[(\Delta\varphi_s)^\infty - (\Delta\varphi_s)_{\Delta I=0}^\infty]/(\Delta I/I_0) \simeq 5.5$. $(\Delta\varphi_s)_{\Delta I}^{100} - (\Delta\varphi_s)_{\Delta I=0}^{100}$ is plotted against ΔI . The MUS apparently shows its linear dependence as anticipated from the theoretical prediction. Their magnitudes agree with each other within a factor of 1.8. Here is again a notable peculiarity of the coefficient α . As has been seen in Figure

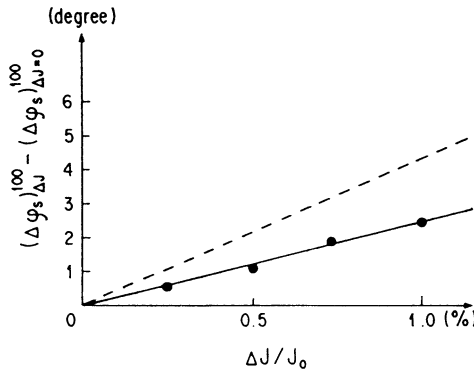


FIGURE 4 Deviation in $(\Delta\varphi_s)^n$ vs. current error; the solid line represents the result of the MUS and the broken line is the theoretical prediction.

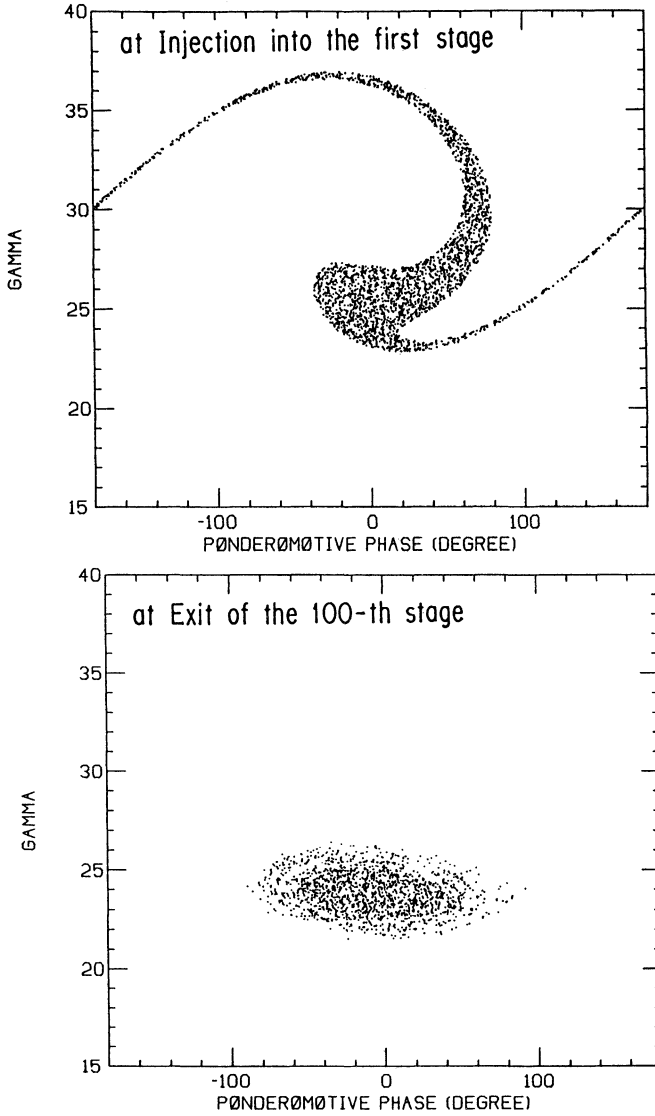


FIGURE 5 Bunch shape at the entrance into the first stage and at the exit of the 100th stage.

2, α is a function of the input power; roughly proportional to $-\sqrt{P(0)}$. A large input power is apparently advantageous to minimize the sensitivity of output RF phase to the injection error.

5 DISCUSSIONS

Energy deviation in a high energy linac due to phase error may be described by $-\frac{1}{2}[(\Delta\phi_s)_{\Delta I} - (\Delta\phi_s)_{\Delta I=0}]^2$. The size of acceptable energy deviation¹¹ mainly depends

on the design of the final focus. If it is typically 0.5%, the output RF phase jitter must be less than 5.7° . Fortunately, the theoretical prediction (19) and extensive MUS have indicated that this requirement can be satisfied with a well bunched beam with a small current error ($\leq 1\%$) and a large input RF power ($\geq \text{MW}$).

There is another aspect on the RF phase's sensitivity to injection errors in a more realistic situation that must be considered, because it seems impossible to produce a perfectly matched beam with a buncher wiggler of finite length. In Figure 5 typical bunch shapes are shown at injection into the first period and at exit of the 100th period. In these MUS¹² one third of injected particles was lost through early 20 stages. Figure 6 shows the output phase ($\Delta\phi_s$)ⁿ and trapping ratio versus the stage number for the case of designed current and the case with current error of 0.5%. For both cases, the large change in $\Delta\phi_s$ at early stages apparently arises from the rapid substantial current loss. Noteworthy is the fact that they reach an equilibrium state beyond the 20th stage where the number of trapped particles almost saturates with the same trapping ratio. This is completely consistent with the qualitative prediction by the theoretical model. The extension of the present model to the transient region, however, poses formidable difficulties for theoretical analysis. The magnitude of cumulative $\Delta\phi_s$ deviation in the example through the entire stage, 4° , is close to the limit. We have observed that a large fraction of it is generated in the transient region. To reduce the sensitivity to injection errors there, a long buncher FEL would be helpful.

Results of the present theory and that given in Ref. 5 are not compared because both theories have been developed in different regimes. The present theory has been applied to the *maximal power extraction regime* where the wiggler length is adjusted to produce the almost maximum RF power at its end. The other has chosen its

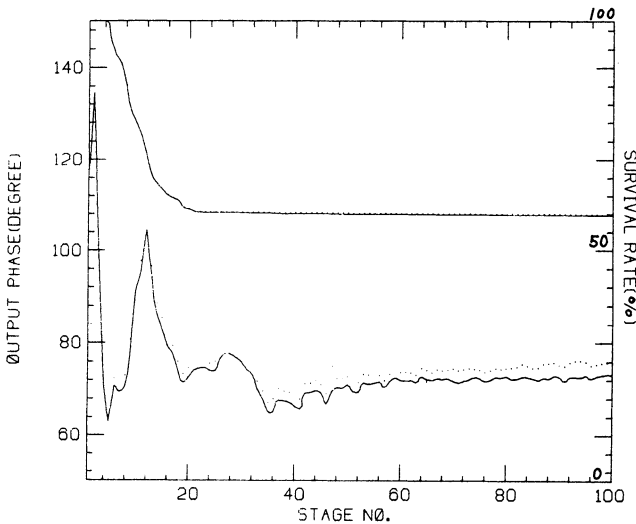


FIGURE 6 Output phase evolution ($\Delta\phi_s$)ⁿ and trapping ratio vs. the stage number; the solid and dotted lines represent the cases of $\Delta I/I_0 = 0$ and $\Delta I/I_0 = 0.5\%$.

application in the *over-rotation regime* where the wiggler is much elongated so as to provide sufficient bunch-rotation in the RF bucket.

6 CONCLUSION

A simple theoretical model for the spatial evolution of the MP and RF signal has been presented which can manifest the output RF phase's sensitivity to the injection error and its FEL parameter dependence, particularly the input power dependence. As a result of theoretical and numerical studies on the RF phase drift, an example of gigantic K-band RF source with output power of 600 MW/m and total length of 150 m¹³ was demonstrated with the acceptable phase sensitivity for 100 multistage, provided well bunched beams. The importance of the detrapped fraction in a more realistic situation was pointed out and the necessity of a complete buncher FEL was suggested to mitigate the effects of the injection current error.

ACKNOWLEDGEMENTS

Discussions with Drs. Sessler and Whittum of LBL and Dr. Wurtele of MIT have stimulated the author to study the present work. The last stage of this work was supported by the U.S. Department of Energy under Contract No. DE-FG05-87ER40374.

REFERENCES

1. A. M. Sessler, in *Laser Acceleration of Particles*, ed. P. J. Channel, AIP Proceedings **91** (New York 1982), 163.
2. A. M. Sessler, E. Sternbach, and J. S. Wurtele, *Nucl. Inst. and Meth.* **B40/41**, 1064 (1989).
3. K. Takayama, *Phys. Rev. Lett.* **63**, 516 (1989).
4. K. Goren and A. M. Sessler, CERN Report 87-11 231 (1987).
5. A. M. Sessler, D. H. Whittum, and J. S. Wurtele, *Part. Accel.* **31**, 69 (1990).
6. S. Hiramatsu, K. Ebihara, Y. Kimura, J. Kishiro, T. Ozaki, K. Takayama, and H. Kurino, *Part. Accel.* **31**, 75 (1990).
7. Multiparticle simulations have been done by numerically integrating the standard FEL equations (the so-called KMR eqs.) for 1716 particles, assuming a single TE_{01} mode. For simplicity, a drift space for energy recovery etc. is ignored in simulations. The continuity of the beam phase at boundary is imposed. The initial RF signal phase is adjusted in such a manner as mentioned in text.
8. N. M. Kroll, P. L. Morton, and M. N. Rosenbluth, *IEEE J. Quantum Electron.* **17**, 1436 (1981) and D. Prosnitz, A. Szoke, and V. K. Neil, *Phys. Rev.* **A24**, 1436 (1981).
9. For the consistency between the recursion model and exact system, the magnitude of $a_w(0)$ used in the MPA is slightly so adjusted that the second term of (9a) is equal to the designed value, that is, $\Delta\gamma + (e/mc^2)/(P(0)/I_0)$ for the other fixed FEL and beam parameters. The difference from the corresponding value used in the MUS is within 2.5%.
10. A. M. Sessler and D. H. Whittum, private communications (1989).
11. S. Hiramatsu, presented at the 2nd Int. Workshop on a Linear Collider 1990, KEK Japan, KEK Internal 90-22.
12. An unmatched beam bunch consisting of 3000 particles which has been generated from the 3 m long buncher wiggler is simulated in the same manner as that of Ref. 8.
13. The drift space of 0.8 m per period is reserved for energy recovery, injection and RF extraction.